

Low symmetry monoclinic M_C phase in epitaxial BiFeO_3 thin films on LaSrAlO_4 substrates

Zuhuang Chen,¹ Zhenlin Luo,² Yajun Qi,¹ Ping Yang,³ Shuxiang Wu,⁴ Chuanwei Huang,¹ Tom Wu,⁴ Junling Wang,¹ Chen Gao,² Thirumany Sritharan,^{1,a)} and Lang Chen^{1,b)}

¹School of Materials Science and Engineering, Nanyang Technological University, Singapore 639798

²Department of Materials Science and Engineering and National Synchrotron Radiation Laboratory, University of Science and Technology of China, Hefei, Anhui 230029, People's Republic of China

³Singapore Synchrotron Light Source (SSLS), National University of Singapore, 5 Research Link, Singapore 117603

⁴Division of Physics and Applied Physics, School of Physical and Mathematical Sciences, Nanyang Technological University, Singapore 637371

(Received 27 October 2010; accepted 17 November 2010; published online 13 December 2010)

We reported that the tetragonal-like phase identified in strained epitaxial BiFeO_3 films on a (001) LaSrAlO_4 single crystal substrates is monoclinic M_C , based on high resolution synchrotron x-ray studies and piezoresponse force microscopy measurements. This M_C phase has different symmetry with the rhombohedral-like monoclinic M_A phase found in BiFeO_3 films grown on low mismatch SrTiO_3 substrates. Transmission electron microscopy revealed that the films on LaSrAlO_4 substrates have a high crystalline quality and coherent interface. © 2010 American Institute of Physics. [doi:10.1063/1.3525378]

Monoclinic phases have been found in lead-based ferroelectrics for compositions around the morphotropic phase boundaries (MPB).^{1,2} These low symmetry phases act as the structural bridges between rhombohedral and tetragonal phases and are considered to be responsible for enhanced piezoelectric properties because of symmetry-allowed polarization rotation.³ Three kinds of ferroelectric monoclinic phases have been reported, namely, M_A , M_B , and M_C , following the notation of Vanderbilt and Cohen.⁴ Among them, the former two belong to the space group Cm and the latter belongs to Pm .⁴ For the M_A/M_B phases, the unit cell is double and is rotated by 45° about the c axis with respect to the pseudocubic cell, and the polarization (P) is confined to lie in the $(1\bar{1}0)$ plane (throughout this letter, pseudocubic index is used). The M_A and M_B unit cells are similar but the magnitudes of their polarization components corresponding to the pseudocubic unit cell are different: for M_A , $P_x = P_y < P_z$, whereas for M_B , $P_x = P_y > P_z$. For the M_C phase, the unit cell is primitive with a unique b_m axis that is oriented along the pseudocubic $[010]$ and the polarization is constrained to lie within the (010) plane. The unit cell parameters for the M_A and M_C phases are shown in Fig. 1(a). These two types of monoclinic phases can be distinguished by x-ray reciprocal space mapping (RSM).^{5,6} For instance, the $(h0l)$ reflection splits into two peaks for the M_A phase, whereas it splits into three peaks for the M_C phase, as shown in Fig. 1(b).

Lead-free BiFeO_3 (BFO) has been extensively studied in the past decade due to its room-temperature multiferroic and superior ferroelectric properties.^{7,8} For device application, BFO is made in thin film form and is thus subjected to strain resulting from the mismatch in lattice parameters between the film and the substrate.⁹ Such substrate-induced strain is recognized as an effective tool to modify the structure and

even tune the physical properties.¹⁰ For example, BFO films under small compressive strain reportedly adopt a rhombohedral-like (R-like) monoclinic M_A phase (space group Cm or Cc , depending on whether the oxygen octahedra rotations are suppressed by the substrate or not, respectively).^{11,12} Recent experimental and theoretical studies have reported that a metastable tetragonal-like (T-like)

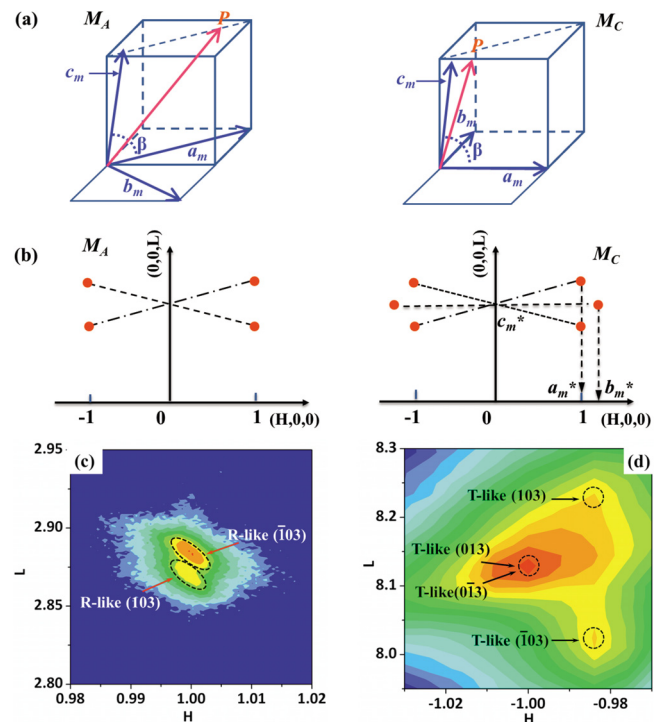


FIG. 1. (Color online) Illustrations of the (a) unit cell parameters related to the pseudocubic unit cell and (b) domain configuration in the reciprocal $(h0l)$ plane for the M_A and M_C phases. The red lines represent the directions of the spontaneous polarization P . (c) X-ray RSM around the 103 reflection of the R-like phase in the film on STO substrate. (d) Synchrotron XRD RSM for the film on LSAO near the $\bar{1}03$ reflection of the T-like phase.

^{a)}Electronic mail: assritharan@ntu.edu.sg.

^{b)}Electronic mail: langchen@ntu.edu.sg.

phase with large tetragonal ratio ($c/a \sim 1.23$) can be stabilized^{13,14} and a MPB-like behavior has been observed in BFO films grown on substrates with lattice mismatches exceeding -4% .^{15,16} Despite these recent advances, the lattice and domain structures of the strain-driven MPB-like system are still unclear. Early first-principles calculations of the strain-induced iso-symmetric Cc - Cc (M_A - M_A) phase transition are believed to be oversimplified.^{17,18} Since the structure of the film plays a crucial role in the physical properties, especially the piezoelectric performance, a thorough investigation of the crystal and domain structures is needed.

In this letter we reveal that the lattice structure of the T-like phase obtained in strained epitaxial BFO films on (001) LaSrAlO₄ (LSAO) single crystal substrates is monoclinic M_C rather than M_A -type as reported in previous studies.^{13-15,19,20} This is based on high resolution synchrotron RSM and piezoresponse force microscopy (PFM) studies. The corresponding ferroelectric domain structure of this strain-driven MPB-like system was also constructed with the aid of PFM images. The polarization vectors of the tetragonal-like phase lie in the (100) plane.

Epitaxial BFO films were grown on (001) oriented LSAO and SrTiO₃ (STO) single crystal substrates by pulsed laser deposition with a KrF excimer laser ($\lambda = 248$ nm). The deposition temperature and the oxygen pressure were 700 °C and 100 mTorr, respectively.¹⁶ X-ray diffraction (XRD) studies of BFO films on STO substrates were performed using a Rigaku four-circle x-ray diffractometer. High resolution RSM studies of BFO films on LSAO substrates were taken at beamline BL14B1 of the Shanghai Synchrotron Radiation Facility (SSRF) at a wavelength of 1.2398 Å. The RSM is plotted in reciprocal lattice units (rlu) of the substrate ($1 \text{ rlu} = 2\pi/3.756 \text{ Å}^{-1}$, in plane, $1 \text{ rlu} = 2\pi/12.636 \text{ Å}^{-1}$, out of plane, for LSAO; $=2\pi/3.905 \text{ Å}^{-1}$ for STO). PFM investigations were carried out on an Asylum Research MFP-3D atomic force microscope (AFM). Transmission electron microscopy (TEM) studies were performed using a JEOL 2100F microscope operating at 200 kV. The TEM cross sectional samples were prepared by mechanical polishing and finally, ion beam polishing.

Our previous study demonstrated the coexistence of T-like and R-like phases in BFO films on LSAO substrate via XRD and AFM measurements.¹⁶ To better differentiate between the T-like and R-like phases, XRD mesh scans are performed in this study around the ($h0l$) reflection. As evident in Fig. 1(c), BFO film on STO shows the expected splitting of the 103 reflection only into two peaks in the diffraction pattern, typical for R-like phase with the M_A structure, which is in agreement with previous reports.^{21,22} Figure 1(d) shows the high resolution synchrotron XRD RSM around the $\bar{1}03$ reflection of the T-like phase of BFO film on LSAO. In contrast to the film on STO, it is found that the $\bar{1}03$ reflection of the T-like phase splits into three adjacent peaks as a consequence of the existence of four domains: one peak is shifted up and another is shifted down with respect to the central peak. This result indicates that the T-like phase must be the monoclinic M_C phase and not the M_A phase. The monoclinic lattice parameters extracted from the $\bar{1}03$ RSM are $a_m = 3.817$ Å, $b_m = 3.756$ Å, $c_m = 4.664$ Å, and $\beta = 88.12^\circ$. This M_C phase is similar to that found in the relaxor ferro-

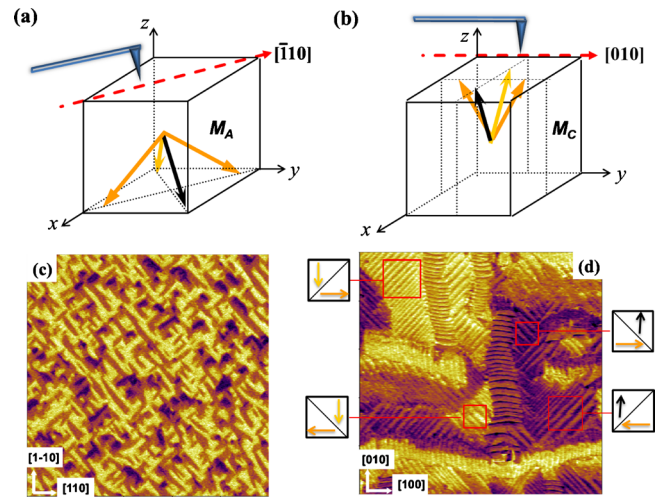


FIG. 2. (Color online) Schematics of the four different domain variants in the monoclinic (a) M_A and (b) M_C phases. The scanning direction of atomic force microscopy cantilever is sketched as well. Arrows represent the polarization directions. (c) In-plane PFM images of BFO films on STO substrate taken with the cantilever along $[110]$ direction. (d) In-plane PFM images of BFO films on LSAO substrate taken with the cantilever along $[100]$ direction; the domain orientations of the T-like phase are indicated in four different areas in red squares. All PFM images are $5 \times 5 \mu\text{m}^2$.

electric $(1-x)\text{PbZn}_{1/3}\text{Nb}_{2/3}\text{O}_3-x\text{PbTiO}_3$ near the MPB composition.²

We also employ PFM to reveal the lattice and domain structures of films and to distinguish the M_C phase from the M_A phase. For M_A and M_C phases, the polarization vectors lie in the $(1\bar{1}0)$ and (010) planes, respectively.^{4,5} In general, monoclinic symmetry gives rise to a very complicated domain structure due to many possible domain states. Epitaxial strain can reduce the number of domain states to four, allowing for a simplified domain analysis.¹² The domains with different orientations are separated by domain walls of specified orientations that satisfy the electrical and mechanical boundary conditions. In the case of M_A -type monoclinic phase, all the permissible domain walls intersect the (001) plane in the $\langle 100 \rangle$ direction.²³ On the contrary, in M_C -type monoclinic phase, intersections of domain walls with the (001) plane are directed along the $\langle 110 \rangle$ direction.²³ In order to differentiate between the possible domain variants, in-plane PFM images were taken with the cantilever pointed along the $\langle 110 \rangle$ axes for M_A -type monoclinic phase, and along $\langle 100 \rangle$ axes for M_C -type monoclinic phase, as indicated in Figs. 2(a) and 2(b) respectively. Figures 2(c) and 2(d) show the corresponding in-plane PFM images of the BFO films on STO and LSAO substrates, respectively. Note that three distinct levels of phase contrast are evident in these images. This observation, together with the uniform contrast shown in the out-of-plane PFM images (not shown here) indicate that the domain structure of the BFO films is characterized by four polarization variants, which are in good agreement with our RSM results. By comparing Figs. 2(c) and 2(d), it can be seen that the domain feature of the T-like phase areas in films on LSAO is quite similar with that of the R-like phase obtained in films on STO. The domain walls in T-like phase areas are parallel to the $\langle 110 \rangle$ direction, while it is pointed along the $\langle 100 \rangle$ in the R-like phase in BFO films on STO, which further supports the hypotheses that the T-like phase here should have a different symmetry from that

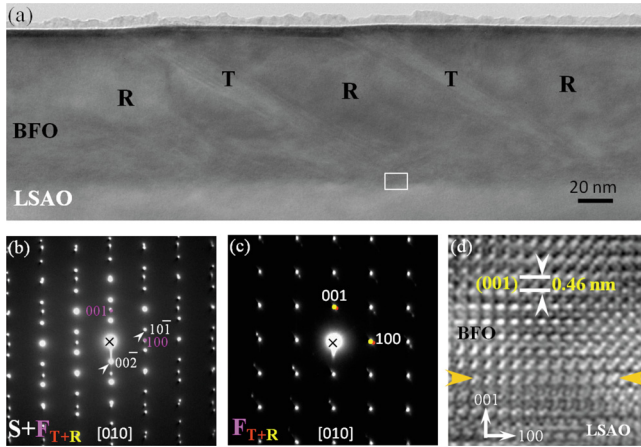


FIG. 3. (Color online) (a) Cross-sectional TEM image of BFO films on LaSrAlO₄ single crystal substrate. “T” and “R” denote the T-like and R-like phase, respectively. (b) SAED pattern taken from an area including both the BFO layer and the substrate. (c) SAED pattern taken from an area including T and R phases in BFO layer. (d) Cross-sectional HRTEM image taken from the rectangle area in (a) showing the BFO/LSAO interface.

of the R-like phase. The observed domain structure of the T-like phase in BFO film on LSAO shown in Fig. 2(d) fits the prediction of Bokov²³ for the M_C phase very well which further supports our suggestion that the M_C phase is present instead of M_A , while the stripe domains observed in BFO films on STO is along $\langle 100 \rangle$ direction, as shown in Fig. 2(c), which is consistent with the previous studies.^{24,25}

The epitaxial and crystalline quality of the films on LSAO substrates were also studied by TEM. Figure 3(a) shows a cross-sectional TEM bright field image of a BFO film on LSAO. The film is about 90 nm thick. As indicated, the film consists of alternating T- and R-like phases. A lower fraction of the T-like phase is evident in the aerial fraction of the TEM cross-section, compared to what could be deduced from AFM topography and XRD pattern.¹⁶ This difference could be due to the strain-relaxation during TEM sample preparation. Figure 3(b) shows selected-area electron diffraction (SAED) pattern along $[010]$ zone axis, which was taken from both the film and the substrate. It shows a combination of patterns from $[010]$ BFO and $[010]$ LSAO with the same $[001]$ direction. The SAED pattern in Fig. 3(c) taken from the film only shows the clear splitting of spots indicated by red and yellow points, corresponding to T- and R-like phases, respectively. Figure 3(d) shows the high-resolution transmission electron microscopy (HRTEM) image obtained from the interface area marked by a rectangle in Fig. 3(a). It is clear that the interface is coherent without any misfit dislocations in this region, confirming a high epitaxy and crystallinity of the film. Thus, SAED and HRTEM results reveal that this BFO film was epitaxially grown on LSAO substrate. Their orientation relations are $(001) \text{ BFO} \parallel (001) \text{ LSAO}$ and $[010] \text{ BFO} \parallel [010] \text{ LSAO}$.

In conclusion, our experimental results suggest that the T-like phase of BFO on LSAO is monoclinic M_C , which is different from M_A type monoclinic phase reported in films grown on low misfit STO substrates. The presence of this low symmetry phase M_C , its linkage to M_A , and the low symmetry monoclinic M_A/M_C multiphases coexistence may give rise to the huge piezoelectric responses for BFO on

LSAO. In addition, the increased variety of domains and phase symmetries could add more tunable functionalities associated with enhanced multiferroicity for BFO films mediated by epitaxial strains.

L.C. acknowledges the support from Nanyang Technological University and Ministry of Education of Singapore under Project No. AcRF RG 21/07 and ARC 16/08. The authors thank beamline BL14B1 (SSRF) for providing the beam time.

- ¹B. Noheda, D. E. Cox, G. Shirane, J. A. Gonzalo, L. E. Cross, and S. E. Park, *Appl. Phys. Lett.* **74**, 2059 (1999).
- ²B. Noheda, D. E. Cox, G. Shirane, S. E. Park, L. E. Cross, and Z. Zhong, *Phys. Rev. Lett.* **86**, 3891 (2001).
- ³H. Fu and R. E. Cohen, *Nature (London)* **403**, 281 (2000).
- ⁴D. Vanderbilt and M. H. Cohen, *Phys. Rev. B* **63**, 094108 (2001).
- ⁵F. M. Bai, N. G. Wang, J. F. Li, D. Viehland, P. M. Gehring, G. Y. Xu, and G. Shirane, *J. Appl. Phys.* **96**, 1620 (2004).
- ⁶G. Y. Xu, H. Hiraka, G. Shirane, J. F. Li, J. L. Wang, and D. Viehland, *Appl. Phys. Lett.* **86**, 182905 (2005).
- ⁷J. Wang, J. B. Neaton, H. Zheng, V. Nagarajan, S. B. Ogale, B. Liu, D. Viehland, V. Vaithyanathan, D. G. Schlom, U. V. Waghmare, N. A. Spaldin, K. M. Rabe, M. Wuttig, and R. Ramesh, *Science* **299**, 1719 (2003).
- ⁸G. Catalan and J. F. Scott, *Adv. Mater.* **21**, 2463 (2009).
- ⁹R. Ramesh and N. A. Spaldin, *Nature Mater.* **6**, 21 (2007).
- ¹⁰D. G. Schlom, L. Q. Chen, C. B. Eom, K. M. Rabe, S. K. Streiffer, and J. M. Triscone, *Annu. Rev. Mater. Res.* **37**, 589 (2007).
- ¹¹H. W. Jang, S. H. Baek, D. Ortiz, C. M. Folkman, R. R. Das, Y. H. Chu, P. Shafer, J. X. Zhang, S. Choudhury, V. Vaithyanathan, Y. B. Chen, D. A. Felker, M. D. Biegalski, M. S. Rzechowski, X. Q. Pan, D. G. Schlom, L. Q. Chen, R. Ramesh, and C. B. Eom, *Phys. Rev. Lett.* **101**, 107602 (2008).
- ¹²C. J. M. Daumont, S. Farokhipoor, A. Ferri, J. C. Wojdel, J. Íñiguez, B. J. Kooi, and B. Noheda, *Phys. Rev. B* **81**, 144115 (2010).
- ¹³H. Béa, B. Dupe, S. Fusil, R. Mattana, E. Jacquet, B. Warot-Fonrose, F. Wilhelm, A. Rogalev, S. Petit, V. Cros, A. Anane, F. Petroff, K. Bouzehouane, G. Geneste, B. Dkhil, S. Lisenkov, I. Ponomareva, L. Bellaiche, M. Bibes, and A. Barthelémy, *Phys. Rev. Lett.* **102**, 217603 (2009).
- ¹⁴A. J. Hatt, N. A. Spaldin, and C. Ederer, *Phys. Rev. B* **81**, 054109 (2010).
- ¹⁵R. J. Zeches, M. D. Rossell, J. X. Zhang, A. J. Hatt, Q. He, C. H. Yang, A. Kumar, C. H. Wang, A. Melville, C. Adamo, G. Sheng, Y. H. Chu, J. F. Ihlefeld, R. Erni, C. Ederer, V. Gopalan, L. Q. Chen, D. G. Schlom, N. A. Spaldin, L. W. Martin, and R. Ramesh, *Science* **326**, 977 (2009).
- ¹⁶Z. H. Chen, L. You, C. W. Huang, Y. J. Qi, J. L. Wang, T. Sritharan, and L. Chen, *Appl. Phys. Lett.* **96**, 252903 (2010).
- ¹⁷Z. H. Chen, Z. L. Luo, C. H. Huang, Y. J. Qi, P. Yang, L. You, C. S. Hu, T. Wu, J. L. Wang, C. Gao, T. Sritharan, and L. Chen, “Low-Symmetry Monoclinic Phases and Polarization Rotation Path Medicated by Epitaxial Strain in Multiferroic BiFeO₃ Thin Films,” *Adv. Funct. Mater.* (in press), DOI 10.1002/adfm.201001867
- ¹⁸J. H. Nam, H. S. Kim, A. J. Hatt, N. A. Spaldin, and H. M. Christen, e-print arXiv:1010.0254.
- ¹⁹B. Dupé, I. C. Infante, G. Geneste, P. E. Janolin, M. Bibes, A. Barthelémy, S. Lisenkov, L. Bellaiche, S. Ravy, and B. Dkhil, *Phys. Rev. B* **81**, 144128 (2010).
- ²⁰D. Mazumdar, V. Shelke, M. Iliev, S. Jesse, A. Kumar, S. V. Kalinin, A. P. Baddorf, and A. Gupta, *Nano Lett.* **10**, 2555 (2010).
- ²¹H. Toupet, F. Le Marrec, C. Lichtensteiger, B. Dkhil, and M. G. Karkut, *Phys. Rev. B* **81**, 140101 (2010).
- ²²Y. H. Chu, T. Zhao, M. P. Cruz, Q. Zhan, P. L. Yang, L. W. Martin, M. Huijben, C. H. Yang, F. Zavaliche, H. Zheng, and R. Ramesh, *Appl. Phys. Lett.* **90**, 252906 (2007).
- ²³A. A. Bokov and Z. G. Ye, *J. Appl. Phys.* **95**, 6347 (2004).
- ²⁴Y. H. Chu, Q. Zhan, L. W. Martin, M. P. Cruz, P. L. Yang, G. W. Pabst, F. Zavaliche, S. Y. Yang, J. X. Zhang, L. Q. Chen, D. G. Schlom, I. N. Lin, T. B. Wu, and R. Ramesh, *Adv. Mater.* **18**, 2307 (2006).
- ²⁵N. Balke, S. Choudhury, S. Jesse, M. Huijben, Y. H. Chu, A. P. Baddorf, L. Q. Chen, R. Ramesh, and S. V. Kalinin, *Nat. Nanotechnol.* **4**, 868 (2009).